Intraband absorption of infrared radiation in a semiconductor quantum dot

V. Milanović
Faculty of Electrical Engineering, University of Belgrade, Bulevar Revolucije 73, P.O. Box 816, 11001 Belgrade, Yugoslavia
and High Technical Post Telegraph and Telephone School, Zdravka Čelara 16, Belgrade, Yugoslavia

Z. Ikonić
Faculty of Electrical Engineering, University of Belgrade, Bulevar Revolucije 73, P.O. Box 816, 11001 Belgrade, Yugoslavia
(Received 13 September 1988)

The energy spectrum and bound-bound intraband transitions in semiconductor quantum dots are analyzed. Numerical results for the GaAs-$Al_xGa_{1-x}As$ system indicate that a considerable absorption at a number of distinct wavelengths in the infrared range (~ 7–25 μm) may be obtained, which greatly exceeds free-carrier absorption.

Much attention has recently been focused on zero-dimensional semiconductor structures, called quantum dots (or quantum boxes).[1,2] Due to the fully discrete energy structure, the absorption spectrum, either intraband or interband, is expected here to be a series of discrete lines, which is of interest in the application of this structure in lasers, optical modulators, etc. Most papers[3–5] on this topic deal with interband absorption. Here, we shall consider intraband transitions of the finite-wall quantum dot, specifically the GaAs dot, in the $Al_xGa_{1-x}As$ matrix.

An eigenfunction of Schrödinger's equation (we use the envelope-function effective-mass approximation) can be separated into radial and angular parts as $[X(r)/r]Y_{lm}(\theta,\phi)$, and the radial part satisfies

$$-\frac{\hbar^2}{2m^*}X''+\left[U(r)+l(l+1)\frac{\hbar^2}{2m^*r^2}\right]X=EX\ , \qquad (1)$$

being valid in the regions $(0,R)$ and $(R,+\infty)$ separately, with appropriate values of the effective mass m^*. The boundary conditions at the interface may be shown to be (see Fig. 1)

$$\frac{1}{m_1}\frac{d}{dr}\left[\frac{X}{r}\right]\bigg|_{r=R^-}=\frac{1}{m_2}\frac{d}{dr}\left[\frac{X}{r}\right]\bigg|_{r=R^+},$$

$$X(R^-)=X(R^+)\ . \qquad (2)$$

In (1), $U(r)$ is the potential energy, which is taken here to have a rectangular shape as in Fig. 1, i.e., space-charge effects are neglected because they are not expected to introduce any qualitative effects. Also depicted in Fig. 1 is the shape of the effective potential [the expression in large parentheses in (1)] for values of the azimuthal quantum number $l=0,1,2$. Obviously, the discrete part of the energy spectrum lies in the interval $[E_{\min}(l),U_0]$, where $E_{\min}(l)=\hbar^2 l(l+1)/(2m_1R^2)$; therefore, there is a maximal l permitting bound levels to exist and may be shown to be

$$l_{\max}=\mathrm{int}[-0.5+0.5(1+4w)^{1/2}],$$

$$w=2m_1R^2U_0/\hbar^2\ . \qquad (3)$$

With rectangular $U(r)$, wave functions may be expressed through Bessel or Hankel functions with boundary conditions (3) and $X(0)=X(+\infty)=0$, as usual.[6]

We also note that the number of bound levels N_b is largest for $l=0$, and may be determined as follows. Defining

$$k_1^2=2m_1E/\hbar^2,\quad k_2^2=2m_2(U_0-E)/\hbar^2\ ,$$

$$f(E)=k_1R/[1-m_1(1+k_2R)/m_2]\ ,$$

and

$$y=\mathrm{int}(2k_1R/\pi)\ ,$$

we have $N_b=(y+1)/2$ for odd y and $N_b=y/2+\varepsilon$ for even y, where ε is equal to zero if $\tan[(2m_1U_0)^{1/2}R/\hbar]\geq f(U_0)$, and $\varepsilon=1$ otherwise. Note that for $m_1=m_2$, $\varepsilon=0$ because $f(U_0)\to-\infty$. For $l\neq 0$,

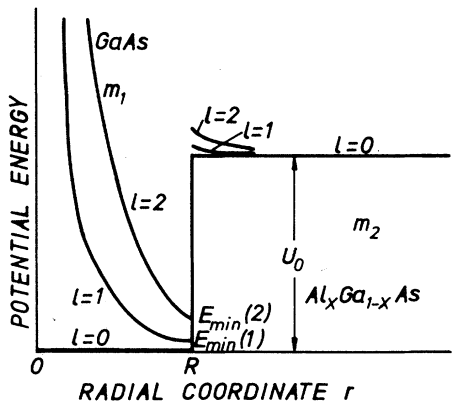

FIG. 1. Effective potential of quantum dot with radius R for values of azimuthal quantum number $l=0$, 1, and 2.

however, no explicit expression for N_b can be derived.

We shall specialize here to electron intraband transitions between bound levels with energies E_i and E_f corresponding to the values of radial, azimuthal, and magnetic quantum numbers $n_{i,f}$, $l_{i,f}$, and $m_{i,f}$, respectively. The transition rate w_{if} is given by the Fermi "golden rule"

$$w_{if}=\frac{2\pi}{\hbar}\sum_{m_i=-l_i}^{m_i=l_i}\sum_{m_f=-l_i}^{m_f=l_i}|P_{i,f}|^2\delta(E_f-E_i-\hbar\omega)\times F_{\mathrm{FD}}(E_i,E_f)\ , \tag{4}$$

where $F_{\mathrm{FD}}(E_i,E_f)$ is the difference of Fermi-Dirac distribution functions for E_i and E_f. The transition matrix element $P_{i,f}$ is equal to $\langle\theta_i|\hat{H}|\theta_f\rangle$, where $\theta_{i,f}$ are the complete electron wave functions, and $\hat{H}=e\,\mathbf{A}\cdot\mathbf{p}/m_0$ ($\mathbf{A}$ is the magnetic vector potential, $\mathbf{p}$ is the momentum operator, and m_0 is the free-electron mass). Following the conventional procedure, the expression for P_{if} may be reduced to

$$P_{i,f}=\frac{e}{i\hbar}(E_i-E_f)\int\int\int\psi_i^*\,\mathbf{A}\cdot\mathbf{r}\psi_f r^2\sin\theta\,d\theta\,d\phi\,dr\ , \tag{5}$$

where ψ_i and ψ_f are the corresponding wave functions. As shown in, e.g., Ref. 7, only transitions with $l_i-l_f=\pm1$ are allowed, and the transition rate takes the form

$$w_{if}=\frac{2\pi}{\hbar}e^2\omega^2A^2|\langle X_i|r|X_f\rangle|^2F_{\mathrm{FD}}(E_i,E_f)q(l_i)\ ,$$
$$q(l_i)=\begin{cases}l_i/3, & l_i-l_f=1\\ (l_i+1)/3, & l_i-l_f=-1\ .\end{cases} \tag{6}$$

The absorption coefficient $\alpha_{i,f}^S$ due to the presence of a single quantum dot in an infinite matrix is given by

$$\alpha_{i,f}^S=\frac{4\pi e^2q(l_i)}{\varepsilon_0\hbar cn_2}|\langle X_i|r|X_f\rangle|^2\frac{F_{\mathrm{FD}}(E_i,E_f)\hbar\omega}{V}\times\delta(E_f-E_i-\hbar\omega)\ , \tag{7}$$

and obviously tends to zero as matrix volume V increases. However, with N dots present, making a finite concentration $n=N/V$, the absorption coefficient of a such a system is

$$\alpha_{if}=\sigma_{i,f}F_{\mathrm{FD}}(E_i,E_f)\cdot n\ ,$$

where $\sigma_{i,f}$ is the absorption cross section

$$\sigma_{i,f}=\frac{16\pi^2\beta q(l_i)\hbar\omega}{n_2}|\langle X_i|r|X_f\rangle|^2\delta(E_f-E_i-\hbar\omega)\ , \tag{8}$$

where single dots are taken to be separated enough not to interact. In (8), $\beta\cong\frac{1}{137}$ is the fine-structure constant, and n_2 the refractive index of the matrix. In real systems, electron scattering induces finite linewidths (Γ) with profiles typically described by a Lorentzian

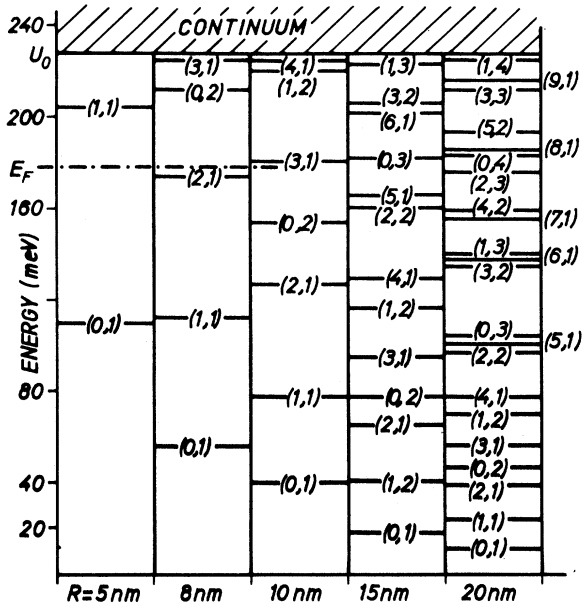

FIG. 2. Energy levels of GaAs quantum dot with radius R embedded in $Al_{0.3}Ga_{0.7}As$ matrix. The first number in parentheses is the azimuthal quantum number l and the second is the radial number n. Also depicted (dashed lines) is the Fermi level E_F corresponding to the doping level of 10^{17} cm^{-3} at $T=300$ K.

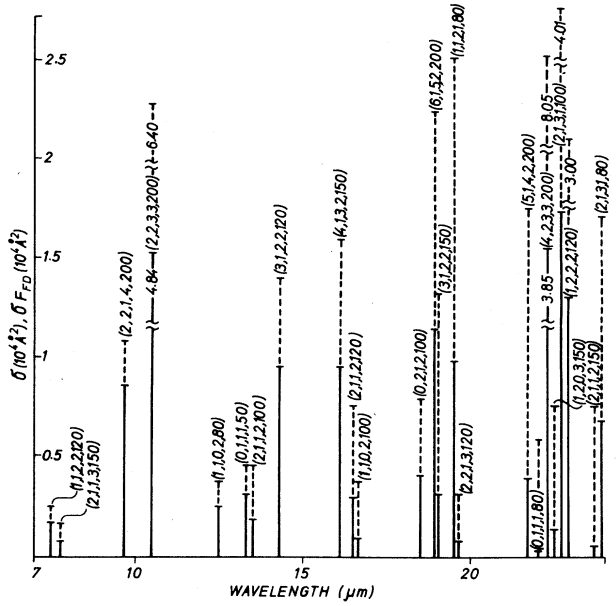

FIG. 3. Values of cross section $\sigma_{i,f}^{\max}$ (dashed lines) and $\sigma_{i,f}^{\max}F_{\mathrm{FD}}$ (solid lines) for a number of transitions in quantum dots of radii R. Numbers in parentheses (l_i,n_i,l_f,n_f,R) R in Å, denote values of azimuthal (l) and radial (n) quantum numbers of initial (i) and final (f) states. Matrix is doped to 10^{17} cm^{-3} and $T=300$ K. Note that where values of $\sigma_{i,f}^{\max}$ or $\sigma_{i,f}^{\max}F_{\mathrm{FD}}$ exceed the scale of figure, the corresponding lines are cut and the corresponding values written along them. The transitions (1,1,0,2,120) and (0,2,1,2,120) at wavelengths 22 and 24 μm and 22 and 28 μm could not be depicted for the sake of clarity, and have $\sigma^{\max}=3776$ Å^2, $\sigma^{\max}F_{\mathrm{FD}}=253$ Å^2, and $\sigma^{\max}=9231$ Å^2, $\sigma^{\max}F_{\mathrm{FD}}=3138$ Å^2, respectively.

$\Gamma/\pi[\Gamma^2+(E_f-E_i-\hbar\omega)^2]$ instead of the δ function in (7) or (8).

Throughout the above considerations, the constancy of the refractive index was assumed. If we take into account the difference between refractive indices of the matrix (n_2) and dot materials (n_1), it turns out that $\langle X_i|r|X_f\rangle$ should be substituted by

$$\langle X_i|r|X_f\rangle \rightarrow \frac{3n_2^2}{n_1^2+2n_2^2}\langle X_i|r|X_f\rangle + \frac{n_1^2-n_2^2}{n_1^2+2n_2^2}\int_R^{+\infty}\left[\frac{R^3}{r^2}+r\right]X_iX_f dr \ . \quad (9)$$

In the GaAs-$Al_xGa_{1-x}As$ system, however, n_1 is close to n_2 and the corresponding correction is small.

Numerical results are presented for the GaAs quantum dot in the $Al_{0.3}Ga_{0.7}As$ matrix. Matrix doping is set at 10^{17} cm^{-3}, which determines the value of the Fermi level E_F. According to the expression for the band-gap difference, $\Delta E_g(x)=1.115x+0.37x^2$ (eV),[8] and assuming 60% of it to be the conduction-band discontinuity, we get $U_0=227$ meV. Energy levels calculated for a couple of dot radii values are given in Fig. 2.

In Fig. 3, values of cross sections $\sigma_{i,f}^{\max}$ (at center of line, $\hbar\omega=E_f-E_i$) with Γ in Lorentzian set at 1 meV for reference, for a number of transitions whose wavelengths are less than 25 μm, are given. Transitions with lower energies can hardly be expected to be visible because of large free-electron absorption of the matrix. Furthermore, we also omitted transitions that are nominally allowed, but have very small σ ($\sigma<500$ Å^2). Along with $\sigma_{i,f}^{\max}$, the values of $\sigma_{i,f}^{\max}F_{FD}$, determining the real absorption, at $T=300$ K and doping level of 10^{17} cm^{-3}, are depicted. Obviously there are transitions that have large $\sigma_{i,f}^{\max}$ but do not accomplish significant absorption, because initial and final states are approximately equally populated. However, these transitions may become very strong for some other set of parameters.

Using the above results one can calculate absorption of a matrix with some definite quantum dot concentration. For example, dots with 200 Å radius may provide absorption of 10.55 μm CO_2-laser radiation at the $(2,2)\rightarrow(3,3)$ transition (Fig. 3). For 2000 Å separation between neighboring dots, a 1-μm-thick sample would absorb $\sim$6% of incident radiation. On the other hand, free-carrier absorption is calculated[9] to be $\sim$0.075%, so absorption on bound-bound transitions is very pronounced and may have applications in quantum electronics.

[1]T. Inoshita, S. Ohnishi, and A. Oshiyama, Phys. Rev. Lett. **57**, 2560 (1986).

[2]H. Watanabe and T. Inoshita, Optoelectron. Dev. Technol. **1**, 33 (1986).

[3]Al. L. Efros and A. L. Efros, Fiz. Tekh. Poluprovdn. **16**, 1209 (1982) [Sov. Phys. — Semicond. **16**, 772 (1982)].

[4]W. Y. Wu, J. N. Schulman, T. Y. Hsu, and U. Efron, Appl. Phys. Lett. **51**, 710 (1987).

[5]S. Schmitt-Rink, D. A. B. Miller, and D. S. Chemla, Phys. Rev. B **35**, 8113 (1987).

[6]S. Flügge, *Practical Quantum Mechanics* (Springer-Verlag, Berlin, 1971), Vol. I, Chap. III D.

[7]V. A. Fock, *Fundamentals of Quantum Mechanics* (Mir, Moscow, 1978), Pt. II, Chap. IV.

[8]S. Adachi, J. Appl. Phys. **58**, R1 (1985).

[9]J. S. Blakemore, J. Appl. Phys. **53**, R123 (1982).